2017

Impacts of climate change and urban growth on the streamflow characteristics of the Milwaukee River (Wisconsin, USA)

Woonsup Choi

Feng Pen

Changshan Wu

This is an Accepted Manuscript of an article published by Springer in Regional Environmental Change in 2017, available online: https://link.springer.com/article/10.1007/s10113-016-1083-3

Title: Impacts of Climate Change and Urban Growth on the Streamflow Characteristics of the Milwaukee River (Wisconsin, USA)

Authors:

Woonsup CHOI (Department of Geography, University of Wisconsin-Milwaukee, wchoi@alumni.illinois.edu)
Feng PAN (Department of Geography, University of Wisconsin-Milwaukee, fengpan@uwm.edu)
Changshan WU (Department of Geography, University of Wisconsin-Milwaukee, cswu@uwm.edu)

Corresponding author: Woonsup CHOI

- Address: Department of Geography, University of Wisconsin-Milwaukee, PO Box 413, Milwaukee, Wisconsin 53201 USA
- Email: wchoi@alumni.illinois.edu
- Phone: +1-414-229-2671

Abstract

Hydrological impact studies of climate change increasingly take land use changes into account. However, the Midwestern USA is still understudied in this context. This study investigated the impacts of potential climate change and urban growth on the streamflow characteristics of the Milwaukee River located in southeastern Wisconsin. The Hydrological Simulation Program-Fortran (HSPF) was set up for the catchment and calibrated against observed streamflow data. The calibrated HSPF model was run with a series of climate and urban growth scenarios generated from nine global climate models (GCMs) and a land use simulation model, respectively. The outcomes from the GCMs, statistically downscaled at 10-km grid spacing, generally indicated a warmer and wetter climate by the mid-21st century, and the land use simulation model projected moderate urban growth by the time. Major findings from the study include: (1) land use changes alone resulted in negligible streamflow changes; (2) low flows showed more sensitivity than mean streamflow to climate change; (3) streamflow variability increased with both land use and climate changes, and (4) uncertainty in simulated streamflow among GCMs was larger than uncertainty among the GCM output themselves. The findings suggest that the current pace of urban growth would not pose much threat to the water resources in the area. Considering that low flow indices responded more sensitively than mean streamflow to climate change, measures to improve resilience to drought conditions are recommended. Because land use change impacts were quite small, considering the impact of both climate and land use scenarios did not produce a significantly different result.

Keywords: *runoff*, *low flow*, *streamflow*, *climate change impact*, *urban growth*

Length: 7823 words

Introduction

In 2013, the atmospheric carbon dioxide concentration surpassed 400 parts per million for the first time in recorded history (http://climate.nasa.gov/climate_resources/24/, last accessed 15 May 2015). The decade of the 2000s was the warmest one amid the certainty that globally averaged near surface temperatures certainly have increased since the late 19th century (Hartmann et al. 2013). Towards the end of the 21st century, global mean temperatures are likely to continue to rise with unabated greenhouse gas emissions, and global precipitation will likely increase by 1-3% per degree Celsius of global mean surface temperature increase under most scenarios (Collins et al. 2013, Meehl et al. 2007). With such changes in temperature and precipitation projected, supply and demand of water resources will certainly be affected around the globe. Rising temperatures will increase evaporation and need for irrigation, increasing demand while reducing supply. Increasing precipitation has the potential to increase supply, but it depends on the geographical and temporal distribution of precipitation. Rising temperatures are also likely to increase urban water demand (Breyer et al. 2012, Chang et al. 2014, Lee et al. 2015), thus urban development can exacerbate water resources impacts of climate change. Urban development affects not only water demand but also the hydrological cycle via modified land covers and water infrastructure. Therefore, it is imperative that urban development is taken into account in climate change impact studies on water resources.

Many studies have been conducted regarding climate change impacts on water resources at global, regional and local scales, and they are summarized in selected works (Leavesley 1994, Sivakumar 2011, Xu et al. 2005). In the Midwestern United States, temperature is projected to increase across the seasons, and precipitation is projected to increase in winter, spring, and autumn by the middle and late 21st century according to the ensemble of recent climate model projections (Collins et al. 2013). Results from selected works for the Midwestern United States (e.g. Wu et al. 2012, Tavakoli and De Smedt 2012, Jha and Gassman 2014, Qiao et al. 2014, Winter et al. 2015) indicate that even though the ensemble of climate model simulations projects precipitation increases, both increases and decreases are considered for precipitation scenarios, and the resulting streamflow changes go both ways. It should be noted that temperatures are predominantly projected to increase, resulting in enhanced potential evapotranspiration and reduced streamflow.

Considering climatic and land use changes simultaneously for impacts on water resources has become more common in recent years. Because runoff occurs after precipitation interacts with the land surface, changing land surface conditions must be taken into account in climate change impact studies. Of particular interest in the water resources context is urban development because it severely modifies the land surface condition by replacing permeable lands with impervious ones. Impervious land covers prevent infiltration of rainwater, thus reducing recharge of groundwater and enhancing overland flow's amount and speed (Jacobson 2011).

Because the climatic and physiographic conditions of the studied catchments are heterogeneous, such studies often have a local to regional character (van Roosmalen et al. 2009). Some studies (e.g. Choi 2008, Praskievicz and Chang 2011, Castillo et al. 2014) find that projected climate change has greater impacts than projected urban development. This is in part because the extent of urban development in the scenarios is very small. Of note is

that land use change is quite influential at certain locations in the catchment (Castillo et al. 2014). In a study where substantial urban growth is projected by 2050 (Tong et al. 2012), the impact on the mean flow was comparable to those of climate scenarios. For the Wolf Bay catchment in southern Alabama, substantial urban development scenarios do not result in significant mean streamflow changes but rather redistribution of streamflow, whereas wet and dry climate scenarios result in substantial streamflow changes (Wang et al. 2014). Across eastern Massachusetts, streamflow is more sensitive to climate change than urban development whereas nitrogen load is similarly sensitive to both (Tu 2009). Runoff is more influenced by climate change, whereas water quality is more influenced by urban growth (or land use change in general) (e.g. Hoyer and Chang 2014, López-Moreno et al. 2014, Psaris and Chang 2014, El-Khoury et al. 2015).

We find that catchments in the Midwest are understudied and little attention has been paid to the impacts on low flows. In the works that examined catchments in the Midwest, the urban fraction was still too small in scenarios (Choi 2008) or hypothetical climate scenarios were used (Tong et al. 2012). This study is distinguished from previous ones by using fine-resolution distributed climatic and urban growth scenarios to examine the impacts on mean and low flows. The climate scenarios were obtained from multiple global climate models that had been downscaled to 10-km grid spacing. The urban growth scenarios were generated from a model that takes socioeconomic factors into account. The present study integrated the climate and urban growth modeling results to investigate their effects on hydrological variables of the Milwaukee River catchment. Specifically, this study attempted to (1) examine the effects on mean flow and low flow of the climate and urban growth scenarios, and (2) assess the uncertainty arising from the climate models.

Study area

We chose the 2330-km^2 Milwaukee River catchment located in southeastern Wisconsin as our study area (Figure 1A). The southern portion of the catchment is heavily populated and urbanized, with more than 1 million inhabitants. The land cover in the northern portion consists primarily of agricultural land. The catchment's topography is comprised of rolling moraine over bedrock, sloping downward from northwest (inland) to southeast (lakeshore) (Wisconsin Department of Natural Resources 2001). There are three major rivers in the catchment, namely Milwaukee, Menomonee, and Kinnickinnic. The Menomonee and Kinnickinnic rivers merge with the Milwaukee River in downtown Milwaukee (approximately 43°/87°50' in Figure 1A), and the Milwaukee River empties into Lake Michigan. The Milwaukee River, the longest, flows from north and northwest to south, and the Menomonee from northwest to southeast. Both rivers flow through both rural and urban areas. The Kinnickinnic River, the shortest, flows from southwest to northeast through a heavily urbanized area. Detailed information about the U.S. Geological Survey (USGS) streamflow measurement sites shown in Figure 1A is provided in Table 1 of the Electronic Supplementary Material.

The climate of the Milwaukee River catchment is characterized by warm summers and cold winters. The January mean temperature of southeastern Wisconsin during 1971-2000 is −7.3°C, and the July mean temperature is 21.8°C. Average annual precipitation is

approximately 862 mm, with wetter summers and drier winters. Annual mean snowfall is 112.3 cm, with 34 cm in January (Wisconsin State Climatology Office 2007). Mean monthly temperature and precipitation are shown in Figure 1 of the Electronic Supplementary Material.

Mean annual runoff measured during 1915-2008 at the USGS site 04087000 is 219 mm, whereas that measured during 1983-2008 at the site 04087159 is 461 mm (Choi et al. 2016). Such a large difference with the same climate demonstrates the effect of land cover. The seasonal pattern is that runoff is high in spring and low in late summer/early autumn, reflecting atmospheric moisture demand, except for the site 04087159 (U.S. Geological Survey 2015), where runoff is quite consistent from March through September (Figure 2 of Electronic Supplementary Material).

Materials and Methods

The study consisted of administering a hydrological model to simulate water resources variables using a range of climate and land use scenarios. Climate scenarios were obtained from the output of global climate models (GCMs), and land use scenarios were obtained from the output of a land use change model. Details are described in the following subsections.

Water resource variables

The study focused on mean streamflow and low flow indicated by 7Q10 and 7Q2. Mean streamflow was obtained by calculating an average of all daily flow values for the entire simulation period. The 7Q10 is an indicator of low flow widely used in the U.S. as a hydrologically-based design flow, and it refers to the lowest 7-day average flow with a 10 percent probability of it occurring in any given year (i.e. 10-year recurrence interval) (Smakhtin 2001, US EPA 2013). Similarly, the 7Q2 is the lowest 7-day average flow with a 50 percent probability of it occurring in any given year. The selected variables addressed part of the water resources research priorities identified by the Wisconsin Initiative on Climate Change Impacts (2011).

The hydrological model

We employed the Hydrological Simulation Program-Fortran (HSPF) (Duda et al. 2012) to simulate streamflow. We used the version embedded in the U.S. Environmental Protection Agency's Better Assessment Science Integrating point & Non-point Sources (BASINS) Version 4.1 (US EPA 2015). BASINS consists of a suite of interrelated components for performing environmental analysis, including a geographic information system tool and hydrological models. HSPF is capable of simulating both hydrological and water quality variables, and most of the input data are readily available for the US catchments. HSPF was employed for several climate change impact studies that took land use changes into account (e.g. Choi 2008, Chung et al. 2011, Praskievicz and Chang 2011, Tong et al. 2012).

In HSPF, the study area is divided into subcatchments according to topography, and each subcatchment contains pervious and impervious land segments and a stream channel

(and/or a reservoir). Model functions and related parameters are associated with the land segments and stream channels such as the water budget function (pervious and impervious land segments) and the hydraulic behavior function (stream channel). Each function has a list of parameters. For example, the water budget function has parameters such as soil moisture storage capacity, fraction of loss to deep aquifers, and groundwater recession rate. Default parameter values are assigned during the model setup and adjusted during calibration.

HSPF requires hourly meteorological and physiographical data to operate. The software requires a minimum of two types of meteorological data: precipitation and evapotranspiration. When evapotranspiration data is not available, it is estimated using related variables such as air temperature, wind speed, and cloud cover. The meteorological data is available for the continental U.S. from the HSPF website and other sources. For our study, we used wind speed and cloud cover data downloaded from the HSPF website and extracted precipitation and temperature data from the gridded historical daily precipitation and maximum/minimum temperature datasets produced by researchers at the University of Wisconsin-Madison (Serbin and Kucharik 2009). The precipitation and temperature datasets were developed by interpolating weather station data across Wisconsin with about 8-km grid spacing (Figure 1A) for the period 1950-2006. An algorithm in BASINS was used to distribute daily precipitation to hourly values. It uses hourly precipitation data from nearby stations whose daily total is closest to the daily data.

The land use/cover data for the baseline period was obtained from the 2001 National Land Cover Database (NLCD) produced by the USGS at a spatial resolution of 30m × 30m. The NLCD 2001 was derived from satellite imageries from the Multi Resolution Land Characteristics Consortium (Homer et al. 2012). Figure 1B shows the NLCD 2001 clipped for the Milwaukee River catchment. The land cover classes have been aggregated for simplicity, and the aggregated classes were used for HSPF (see Table 2 of Electronic Supplementary Material).

The model parameters were calibrated against the measured streamflow data for the period 1986-1995 and validated for the period 1996-2005. The streamflow data were obtained from the four USGS sites shown in Figure 1A. From north to south in the map, they are referred to as Cedarburg, Milwaukee, Menomonee, and Kinnickinnic, respectively. The selection of the calibration period was based on the availability of the NLCD and streamflow data. The comparison with the measured streamflow included calculation of the relative error (RE) and the Nash-Sutcliffe Efficiency (NSE) (Nash and Sutcliffe 1970). The RE refers to the percentage difference between the simulated mean runoff and the measured mean runoff and indicates the overall offset from observations. The NSE measures goodness-of-fit between the two time series and ranges from $-\infty$ to unity. Unity indicates a perfect fit, and negative numbers indicate that the mean of the measured runoff is a better predictor than the model.

Model evaluation parameters for the calibration and validation periods are presented in Figure 3 of the Electronic Supplementary Material. With the exception of Kinnickinnic, the RE was less than 5%, indicating overall very low offset from observations. NSE values for the calibration period range from 0.62 (Kinnickinnic) to 0.71 (Milwaukee), and they were slightly lower for the validation period across the sites. Overall, the model accurately reproduced the mean streamflow and did a reasonable job with goodness-of-fit.

Climate scenarios

Climate scenarios were derived from a climate model-based dataset created under the Wisconsin Initiative on Climate Change Impacts. The dataset was produced by statistically downscaling the output from nine global climate models (GCMs) (Table 3 of Electronic Supplementary Material) with approximately 10-km grid spacing. Statistical downscaling refers to a procedure that finds statistical relationships between macro-scale atmospheric conditions (such as pressure fields) and micro-scale ground-level measurements (such as near-surface air temperature) in order to transform the coarse-resolution GCM-simulated meteorological variables to the finer resolution needed for the study. The nine GCMs were statistically downscaled using the macro-scale atmospheric data from the National Center for Environmental Prediction/National Center for Atmospheric Research (Kalnay et al. 1996) and ground-level measurements from the National Weather Service's Cooperative Observer Program stations (for details, see Notaro et al. 2011).

The downscaled GCM dataset includes late-20th century simulations (1961-2000) and mid-21st century projections (2046-2065) using the Special Report on Emissions Scenarios A1B greenhouse gas emissions scenario (Nakicenovic and Swart 2000). In this scenario, fossil CO_2 emissions begin to decrease after the mid-21st century, and there is a moderate increase in atmospheric CO_2 concentrations. Of the six SRES emissions scenarios (A1B, A1FI, A1T, A2, B1, and B2), the A1B scenario lies in the middle (Meehl et al. 2007).

The models matched well with the historical data (Table 1). The historical data had slightly higher temperature (7.95°C) than the GCMs (7.8°C) but very similar interannual variability. Its standard deviation was 0.8, and that of GCMs ranged from 0.7 to 1.2. The precipitation from the historical data (816 mm) was in the middle of the GCM data range (792-827 mm), and the interannual variability (standard deviation of 114) was at the lower end (109-222). By the mid-21st century, all the models projected warming of 3-4°C, and most of the models projected wetter climates except two (gfdl_cm2_0 and csiro_mk3_5).

All the GCMs predicted an increase in temperature by 2046-2065 with respect to the monthly baseline (Figure 2); increases were particularly large in December and January, with a median (red lines in the boxes) value of approximately 4°C. Precipitation was generally projected to increase as well by 2046-2065, particularly in the colder months; January and December were the months with the highest increase, with a median value of more than 20%. Regarding the changes between May and November, median values varied around zero.

Land use scenarios

We developed two Cellular Automata (CA)-based models to simulate the spatial dynamics of residential and commercial land uses. CA models are a group of micro-scale urban spatial dynamic simulation models, widely used for simulating urban growth (e.g. Li et al. 2014). The input to the model was the aforementioned 30m × 30m NLCD dataset, and the output was the projected land use/cover grid at the same resolution. The general structure of CA is described as follows:

$$U_i = f(P_i, N_i, C_i, R_i)$$

where U_i is the probability of cell i being converted to developed lands, P_i is the global probability of conversion to developed lands, N_i is the neighborhood effect, C_i is the constraint factor, and R_i represents the random factor.

To calculate the global probability of residential/commercial expansion, a logistic regression model was constructed using driving factors including elevation, slope, distance to the nearest city, distance to lake, distance to railway, distance to river, distance to road, distance to village, and population density. In addition, the neighborhood effect N_i, an essential factor of the CA model, was computed by dividing urban cell numbers within the neighborhood by the entire cell numbers within the neighborhood. As a result, N_i indicates the influence of neighboring land uses on the probability of conversion to developed land use. Two major constraints, water bodies and slopes, were employed in the CA model. In other words, water bodies and lands with a slope of 22.5° or higher were less likely to be developed. Finally, a random factor (R_i) was employed to represent the stochastic characteristics of the urban growth models.

With the collected residential and commercial data for the catchment, we constructed and calibrated the model for the period 1990-2000, and the years 2000-2005 was employed for the model validation. With all identified parameters, the residential and commercial growth models were applied to CA models to simulate residential and commercial growth in 2050 (for the map, see Figure 4 of Electronic Supplementary Material). Results indicated that both the residential and commercial growth models worked well with kappa values of 97.25% and 93.50%, respectively.

The land use change model projected a modest increase (8.25%) in developed lands by the year 2050 (Table 2). Forest, shrubland, and other vegetation land covers were projected to decrease instead. The developed lands showed both largest relative and absolute changes.

Results

The calibrated HSPF model was run with all the climate and land use scenarios (Table 3). We report the results from the simulations by the water resources variables for the entire catchment.

Mean and variability of streamflow

The streamflow results obtained from the different modeling experiments are presented in Table 4, averaged for the entire simulation periods. For Baseline, the smallest flow of 220 m^3/s was simulated with gfdl_cm2_0, and the largest flow of 256.4 m^3/s with csiro_mk3_5. Streamflow from LUC was almost identical to that from Baseline, with no changes larger than 2%, but streamflow changes varied widely between GCMs in CC, from 155 m^3/s (gfdl_cm2_0) to 278.6 m^3/s (giss_model_e_r). The largest and smallest flows also reflected the largest percentage increase (18.3%) and decrease (29.5%), respectively. The different GCMs showed equal possibilities of both increase and decrease in streamflow. The magnitudes of mean streamflow from CLUC were slightly smaller than those from CC, reflecting the small decreases in LUC.

To further examine the land use change impacts, we compared streamflow from each land use type between the two modeling experiments, Baseline and LUC (Table 5). Developed lands were the largest source of streamflow, followed by planted/cultivated. Together they accounted for 78% of total runoff in the Baseline simulation. As a result of the land use change by the 2050s, streamflow from developed lands was projected to increase by 7.79 m^3/s, whereas that from planted/cultivated to decrease by 6.37 m^3/s. Streamflow was projected to decrease for other land use types as well, resulting in net decrease of 1.96 m^3/s (0.7% of the Baseline total).

Mean monthly flow results from the modeling experiments are presented in Figure 3. Baseline streamflow tended to peak in spring and summer and decrease in winter. Streamflow in July showed the largest variability among the GCMs. The seasonal pattern did not change much with the inclusion of land use or climate changes. The results from LUC were almost identical to Baseline because the same GCMs were used. In CC and CLUC, increased inter-model variability was very noticeable. Variability increased across the year, particularly in the months of April, June and October. Regarding the median values, April stood out compared to May and June. Streamflow in April was projected to increase not only with respect to Baseline but also compared to May and June, resulting in more contrast between spring and summer. At the same time, streamflow in July and August was projected to decrease from the Baseline and become less than June and September streamflow.

Figure 4 portrays the probability of exceedence of daily streamflow values from the four hydrological modeling experiments with nine GCMs. In Baseline, the maximum reached approximately 30 000 m^3/s, and the minimum fell below 10 m^3/s at least with some GCMs. The curves diverged from each other towards the lower end of distribution, suggesting large variability in low flow simulations. LUC did not appear to cause noticeable changes in the distribution of daily streamflow. With climate change, the maximum did not appear to exceed 20 000 m^3/s in any GCM, a large decrease from Baseline. The curves diverged more than in Baseline for most of the data range.

Low flow indices

7Q10 showed the smallest variation for Baseline with csiro_mk3_5 (21.1 m^3/s) and the largest variation with giss_model_e_r (44.4 m^3/s) (Table 6 upper panel). The csiro_mk3_5 model resulted in the largest mean flow (256.4 m^3/s) but the smallest 7Q10 of all the GCMs, which indicates larger variability of daily streamflow than other GCMs. For LUC, 7Q10 is projected to change (mostly decrease) more than mean streamflow. LUC was found to result in decreases in the lower end of daily streamflow, even though it was not visible in Figure 4. The largest percentage decrease is projected with csiro_mk3_0 (11.5%), whereas increases are quite small (1.5% with mpi_echam5). Climate change is projected to have very large impacts on 7Q10. 7Q10 is projected to increase by up to 41.9% (giss_model_e_r) and decrease by up to 71.2% (csiro_mk3_5). Increases and decreases of 7Q10 are almost evenly split between the GCMs. The CLUC scenario showed a similar result to CC. The smallest 7Q2 (58.8 m^3/s) was obtained with csiro_mk3_0 and the largest (78.9 m^3/s) with mri_cgcm2_3_2a for Baseline (Table 6 lower panel). In most of the cases 7Q2 was projected to change in the same direction as 7Q10 but generally with smaller percentage changes.

Discussion

The study found negligible impacts of land use change on mean streamflow. The negligible impacts are due to moderate land use change and their offsetting effects on runoff. Runoff increases from urban expansion were offset by runoff decreases from reduction of forest and planted/cultivated lands. In a similar study using HSPF, Praskievicz and Chang (2011) report runoff decreases with the conservation scenario where urban land use slightly increases and open water and wetland increase substantially. Choi and Deal (2008) also report minute increases in mean runoff (~1%) but more substantial increases in surface flow (8.6-38.5%) with modest urban growth scenarios. However, when a scenario of substantial urban expansion was used, runoff was projected to increase by 29% (Tong et al. 2012). Therefore, urban land use increases of just a few percent do not seem to result in noticeable runoff increases.

Unlike land use change impacts, climate change impacts on mean streamflow were quite large with some GCMs. Runoff changes from climate scenarios generally reflect precipitation changes projected by the GCMs (Table 1). Two of the GCMs project precipitation decreases, and runoff is projected to decrease substantially (>19%) with the two GCMs. Other GCMs projecting precipitation increases result in a wide range of runoff changes, from minute decreases to an increase more than 18%, reflecting variable precipitation increases and consistent warming. Inter-GCM variability of precipitation grows in the 21st century and is reflected on the median of daily flow values (Figure 4 lower panel). The inter-GCM variability of streamflow is even more visible at the monthly scale indicated by longer boxes and whiskers in the graph (Figure 3). Overall, there is a wide range in the projected changes of streamflow with climate scenarios, and mean monthly flow is more likely to increase than decrease.

Low flow indicators were found to be more sensitive to climate and land use scenarios than the mean runoff demonstrated by larger percentage changes. The two GCMs resulting in runoff decrease resulted in even more substantial decreases in 7Q10 (67-71%) and 7Q2 (32-59%), suggesting increased variability in daily streamflow. The implication from such a result is a different risk of streamflow drought. Of note is that drought is different from low flows. Droughts generally refer to sustained conditions where water (e.g. precipitation, soil moisture, streamflow, groundwater, etc.) is significantly less available than normal (Mishra and Singh 2010, Van Loon 2015) whereas low flows generally mean streamflow during the dry season of the year (Smakhtin 2001). In the Milwaukee River catchment, the low flow season runs from late summer to winter, and precipitation is lowest in winter. Decreasing low flows mean that flows will be even lower during the low flow season. If this decreased low flow becomes a new "normal", a condition that is considered drought now may not be considered drought in the future. At the same time, a drought condition in the future will have even less amount of water in the river.

Climate change impact studies on hydrology involve uncertainties at every step of research: choice of emissions scenarios, GCM, downscaling methods, and hydrological model. The choice of emissions scenarios and GCMs is considered important sources of uncertainty (Prudhomme et al. 2003, Wilby and Harris 2006), but downscaling methods can cause larger uncertainty than emissions scenarios (Choi et al. 2014). Winter et al. (2015) emphasize using ensemble-based methods of regional climate modeling is

necessary to capture the full range of potential responses of the hydrologic cycle to climate change. Our study used the downscaled GCM data that have been produced for the Wisconsin Initiative on Climate Change Impacts, thus the analysis was conducted within the scope of the data: nine different GCMs for the same emission scenario and downscaling method. The results varied widely by GCMs, in accordance with many existing studies that reported large uncertainties from GCMs.

Conclusions

By the mid-21st century, the Milwaukee River catchment is projected to see a modest growth in urban areas and a warmer and wetter climate. The confidence level for precipitation increase is not as high as that of temperature increase. Urban areas are projected to expand at the expense of mostly forest and agricultural lands. In response to such projected changes in climate and land use conditions, the following impacts on water resources were projected: (1) land use changes alone resulted in negligible hydrological changes; (2) low flows showed more sensitivity than mean streamflow to climate change; (3) streamflow variability increased with both land use and climate changes; and (4) uncertainty in simulated streamflow among GCMs was larger than uncertainty among the GCM output themselves.

The findings suggest that the current pace of urban growth would not pose much threat to the water resources in the area. Therefore, we recommend that local authorities control the pace of urban growth within the projections presented in this study. Considering that low flow indices responded more sensitively than mean streamflow to climate change, measures to improve resilience to hydrological drought conditions, such as early warning systems and improved water use efficiency, are recommended. Because land use change impacts were small, considering the impact of both climate and land use scenarios did not produce a very different result.

Acknowledgement

This work was supported in part under a grant from the U.S. Geological Survey, U.S. Department of Interior, federal grant number G11AP20115, Project 2013WI314B and with funds from the University of Wisconsin-Milwaukee.

References

Breyer B, Chang H, Parandvash GH (2012) Land-use, temperature, and single-family residential water use patterns in Portland, Oregon and Phoenix, Arizona. Appl Geogr 35:142-151. doi: http://dx.doi.org/10.1016/j.apgeog.2012.06.012

Castillo CR, Güneralp İ, Güneralp B (2014) Influence of changes in developed land and precipitation on hydrology of a coastal Texas watershed. Appl Geogr 47:154-167. doi: http://dx.doi.org/10.1016/j.apgeog.2013.12.009

Chang H, Praskievicz S, Parandvash H (2014) Sensitivity of Urban Water Consumption to Weather and Climate Variability at Multiple Temporal Scales: The Case of Portland, Oregon. International Journal of Geospatial and Environmental Research 1: No. 1, Article 7. Available at: http://dc.uwm.edu/ijger/vol1/iss1/7

Choi W (2008) Catchment-scale hydrological response to climate-land-use combined scenarios: A case study for the Kishwaukee River basin, Illinois. Physical Geography 29:79-99. doi: 10.2747/0272-3646.29.1.79 ER

Choi W, Deal BM (2008) Assessing hydrological impact of potential land use change through hydrological and land use change modeling for the Kishwaukee River basin (USA). Journal of Environmental Management, 88:1119-1130. doi: 10.1016/j.jenvman.2007.06.001

Choi W, Nauth K, Choi J, Becker S (2016) Urbanization and Rainfall-Runoff Relationships in the Milwaukee River Basin. The Professional Geographer 68:14-25. doi: 10.1080/00330124.2015.1007427

Choi W, Kim S, Lee M, Koenig K, Rasmussen P (2014) Hydrological Impacts of Warmer and Wetter Climate in Troutlake and Sturgeon River Basins in Central Canada. Water Resour Manage 28:5319-5333. doi: 10.1007/s11269-014-0803-z

Chung E, Park K, Lee KS (2011) The relative impacts of climate change and urbanization on the hydrological response of a Korean urban watershed. Hydrol Process 25:544-560. doi: 10.1002/hyp.7781

Collins M, Knutti R, Arblaster J, Dufresne J-, Fichefet T, Friedlingstein P, Gao X, Gutowski WJ, Johns T, Krinner G, Shongwe M, Tebaldi C, Weaver AJ, Wehner M (2013) Long-term Climate Change: Projections, Commitments and Irreversibility. In: Stocker TF, Qin D, Plattner G-, Tignor M, Allen SK, Boschung J, Nauels A, Xia Y, Bex V, Midgley PM (eds) Climate Change 2013: The Physical Science Basis. Contribution of Working Group I to the Fifth Assessment Report of the Intergovernmental Panel on Climate Change. Cambridge University Press, Cambridge, United Kingdom and New York, NY, USA, pp 1029-1136

El-Khoury A, Seidou O, Lapen DR, Que Z, Mohammadian M, Sunohara M, Bahram D (2015) Combined impacts of future climate and land use changes on discharge, nitrogen and phosphorus loads for a Canadian river basin. J Environ Manage 151:76-86. doi: http://dx.doi.org/10.1016/j.jenvman.2014.12.012

Hartmann DL, Klein Tank AMG, Rusticucci M, Alexander LV, Brönnimann S, Charabi Y, Dentener FJ, Dlugokencky EJ, Easterling DR, Kaplan A, Soden BJ, Thorne PW, Wild M, Zhai PM (2013) Observations: Atmosphere and Surface. In: Stocker TF, Qin D, Plattner G-, Tignor M, Allen SK, Boschung J, Nauels A, Xia Y, Bex V, Midgley PM (eds) Climate Change 2013: The Physical Science Basis. Contribution of Working Group I to the Fifth Assessment Report of the Intergovernmental Panel on Climate Change. Cambridge University Press, Cambridge, United Kingdom and New York, NY, USA, pp 159-254

Homer CH, Fry JA, Barnes CA (2012) The National Land Cover Database U.S. Geological Survey Fact Sheet 2012-3020:4

Hoyer R, Chang H (2014) Assessment of freshwater ecosystem services in the Tualatin and Yamhill basins under climate change and urbanization. Appl Geogr 53:402-416. doi: 10.1016/j.apgeog.2014.06.023

Jacobson CR (2011) Identification and quantification of the hydrological impacts of imperviousness in urban catchments: A review. J Environ Manage 92:1438-1448. doi: 10.1016/j.jenvman.2011.01.018

Jha MK, Gassman PW (2014) Changes in hydrology and streamflow as predicted by a modelling experiment forced with climate models. Hydrol Process 28:2772-2781. doi: 10.1002/hyp.9836

Kalnay E, Kanamitsu M, Kistler R, Collins W, Deaven D, Gandin L, Iredell M, Saha S, White G, Woollen J, Zhu Y, Chelliah M, Ebisuzaki W, Higgins W, Janowiak J, Mo KC, Ropelewski C, Wang J, Leetmaa A, Reynolds R, Jenne R, Joseph D (1996) The NCEP/NCAR 40-year reanalysis project. Bulletin of the American Meteorological Society 77:437-471. doi: 10.1175/1520-0477(1996)077<0437:TNYRP>2.0.CO;2

Leavesley GH (1994) Modeling the Effects of Climate-Change on Water-Resources - a Review. Clim Change 28:159-177. doi: 10.1007/BF01094105

Lee S, Chang H, Gober P (2015) Space and time dynamics of urban water demand in Portland, Oregon and Phoenix, Arizona. Stoch Environ Res Risk Assess 29:1135-1147. doi: 10.1007/s00477-014-1015-z

Li W, Wu C, Zang S (2014) Modeling urban land use conversion of Daqing City, China: A comparative analysis of "top-down" and "bottom-up" approaches. Stochastic Environmental Research and Risk Assessment 28:817-828. doi: 10.1007/s00477-012-0671-0

López-Moreno JI, Zabalza J, Vicente-Serrano SM, Revuelto J, Gilaberte M, Azorin-Molina C, Morán-Tejeda E, García-Ruiz JM, Tague C (2014) Impact of climate and land use change on water availability and reservoir management: Scenarios in the Upper Aragón River, Spanish Pyrenees. Sci Total Environ 493:1222-1231. doi: http://dx.doi.org/10.1016/j.scitotenv.2013.09.031

Meehl GA, Stocker TF, Collins WD, Friedlingstein P, Gaye AT, Gregory JM, Kitoh A, Knutti R, Murphy JM, Noda A, Raper SCB, Watterson IG, Weaver AJ, Zhao Z-C (2007) Global Climate Projections. In: Solomon S, Qin D, Manning M, Chen Z, Marquis M, Averyt KB, Tignor M, Miller HL (eds) Climate Change 2007: The Physical Science Basis. Contribution of Working Group I to the Fourth Assessment Report of the Intergovernmental Panel on Climate Change. Cambridge University Press, Cambridge, UK and New York, USA, pp 747-845

Mishra AK, Singh VP (2010) A review of drought concepts. Journal of Hydrology 391:202-216. doi: 10.1016/j.jhydrol.2010.07.012

Nakicenovic N, Swart R (2000) Special Report on Emissions Scenarios. Cambridge University Press, pp 599

Nash JE, Sutcliffe JV (1970) River flow forecasting through conceptual models part I — A discussion of principles. Journal of Hydrology 10:282-290

Notaro M, Lorenz DJ, Vimont D, Vavrus S, Kucharik C, Franz K (2011) 21st century Wisconsin snow projections based on an operational snow model driven by statistically downscaled climate data. Int J Climatol 31:1615-1633. doi: 10.1002/joc.2179

Praskievicz S, Chang H (2011) Impacts of Climate Change and Urban Development on Water Resources in the Tualatin River Basin, Oregon. Ann Assoc Am Geogr 101:249-271. doi: 10.1080/00045608.2010.544934

Prudhomme C, Jakob D, Svensson C (2003) Uncertainty and climate change impact on the flood regime of small UK catchments. J Hydrol 277:23. doi: 10.1016/S0022-1694(03)00065-9
Psaris M, Chang H (2014) Assessing the Impacts of Climate Change, Urbanization, and Filter Strips on Water Quality Using SWAT. International Journal of Geospatial and Environmental Research 1: No. 2 Article 1. Available at: http://dc.uwm.edu/ijger/vol1/iss2/1
Qiao L, Pan Z, Herrmann RB, Hong Y (2014) Hydrological Variability and Uncertainty of Lower Missouri River Basin Under Changing Climate. J Am Water Resour Assoc 50:246-260. doi: 10.1111/jawr.12126
Serbin SP, Kucharik CJ (2009) Spatiotemporal Mapping of Temperature and Precipitation for the Development of a Multidecadal Climatic Dataset for Wisconsin. Journal of Applied Meteorology and Climatology 48:742-757. doi: 10.1175/2008JAMC1986.1 ER
Sivakumar B (2011) Global climate change and its impacts on water resources planning and management: assessment and challenges. Stochastic Environmental Research and Risk Assessment 25:583-600. doi: 10.1007/s00477-010-0423-y
Smakhtin VU (2001) Low flow hydrology: a review. Journal of Hydrology 240:147-186
Tavakoli M, De Smedt F (2012) Impact of Climate Change on Streamflow and Soil Moisture in the Vermilion Basin, Illinois. J Hydrol Eng 17:1059-1070. doi: 10.1061/(ASCE)HE.1943-5584.0000546
Tong STY, Sun Y, Ranatunga T, He J, Yang YJ (2012) Predicting plausible impacts of sets of climate and land use change scenarios on water resources. Appl Geogr 32:477-489. doi: 10.1016/j.apgeog.2011.06.014
Tu J (2009) Combined impact of climate and land use changes on streamflow and water quality in eastern Massachusetts, USA. Journal of Hydrology 379:268-283. doi: 10.1016/j.jhydrol.2009.10.009
U.S. Geological Survey (2015) Surface Water data for USA: USGS Surface-Water Monthly Statistics. http://waterdata.usgs.gov/nwis/monthly?. Accessed May/19 2015
US EPA (2015) BASINS 4.1 (Better Assessment Science Integrating point & Non-point Sources) Modeling Framework. National Exposure Research Laboratory, RTP, North Carolina. https://www.epa.gov/exposure-assessment-models/basins. Accessed August/22 2016
US EPA (2013) Flow 101. http://water.epa.gov/scitech/datait/models/dflow/flow101.cfm#1Q10. Accessed May 26 2015
Van Loon AF (2015) Hydrological drought explained. Wiley Interdisciplinary Reviews-Water 2:359-392. doi: 10.1002/wat2.1085
van Roosmalen L, Sonnenborg TO, Jensen KH (2009) Impact of climate and land use change on the hydrology of a large-scale agricultural catchment. Water Resources Research 45:W00A15. doi: 10.1029/2007WR006760
Wang R, Kalin L, Kuang W, Tian H (2014) Individual and combined effects of land use/cover and climate change on Wolf Bay watershed streamflow in southern Alabama. Hydrol Process 28:5530-5546. doi: 10.1002/hyp.10057

Wilby RL, Harris I (2006) A framework for assessing uncertainties in climate change impacts: Low-flow scenarios for the River Thames, UK. Water Resources Research 42:W02419, doi:10.1029/2005WR004065
Winter JM, Yeh PJ-, Fu X, Eltahir EAB (2015) Uncertainty in modeled and observed climate change impacts on American Midwest hydrology. Water Resour Res 51:3635-3646. doi: 10.1002/2014WR016056
Wisconsin Department of Natural Resources (2001) The State of the Milwaukee River Basin PUBL WT 704 2001
Wisconsin Initiative on Climate Change Impacts (2011) Wisconsin's Changing Climate: Impacts and Adaptation
Wisconsin State Climatology Office (2007) Historical Climate Data. http://www.aos.wisc.edu/~sco/clim-history/division/4709-climo.html. Accessed May/19 2015
Wu Y, Liu S, Abdul-Aziz OI (2012) Hydrological effects of the increased CO2 and climate change in the Upper Mississippi River Basin using a modified SWAT. Clim Change 110:977-1003. doi: 10.1007/s10584-011-0087-8
Xu CY, Widen E, Halldin S (2005) Modelling hydrological consequences of climate change - Progress and challenges. Adv Atmos Sci 22:789-797. doi: 10.1007/BF02918679

Tables

Table 1. Spatially-averaged mean annual temperature (°C) and precipitation (mm) for 1961-2000 and 2046-2065 from the historical data and downscaled GCMs. Standard deviations across the years are shown in parenthesis. The largest and smallest precipitation values from each period are shown bold.

	1961-2000		2046-2065	
Dataset	Temperature	Precipitation	Temperature	Precipitation
Historical	7.95 (0.8)	816 (114)	N/A	N/A
cccma_cgcm3_1	7.8 (0.9)	814 (146)	11.4 (0.9)	868 (151)
cnrm_cm3	7.8 (1.2)	**792** (137)	11 (0.7)	931 (147)
csiro_mk3_0	7.8 (0.7)	809 (154)	10.1 (0.6)	855 (184)
csiro_mk3_5	7.8 (1.1)	826 (222)	11 (1.3)	804 (225)
gfdl_cm2_0	7.8 (0.7)	**792** (119)	11 (0.8)	**692** (133)
giss_model_e_r	7.8 (0.8)	821 (109)	10.2 (0.5)	**944** (121)
miub_echo_g	7.8 (1.1)	798 (127)	11.9 (1.2)	864 (136)
mpi_echam5	7.8 (0.9)	**827** (159)	10.6 (0.9)	876 (162)
mri_cgcm2_3_2a	7.8 (0.7)	**827** (129)	10.7 (0.6)	893 (115)

Table 2. Land use statistics and projected changes by the year 2050

Land use	Current (km^2)	2050 (km^2)	Change (%)
Water	21.21	20.94	-1.27
Developed	714.28	773.18	8.25
Barren	1.83	1.85	1.09
Forest	240.47	224.48	-6.65
Shrubland	15	14.02	-6.53
Herbaceous	15.87	15	-5.48
Planted/Cultivated	949.56	911.03	-4.06
Wetlands	261.71	259.45	-0.86

Table 3. Hydrological modeling experiment setup consisting of different climate and land use scenarios

Modeling experiments	Acronym	Temperature and precipitation data	Land use data
Baseline	Baseline	Downscaled 1961-2000	2000
Land use change only	LUC	Downscaled 1961-2000	2050
Climate change only	CC	Downscaled 2046-2065	2000
Climate and land use changes	CLUC	Downscaled 2046-2065	2050

Table 4. Simulated streamflow (m^3/s) from different modeling experiments, averaged for the entire simulation periods. Percentage changes from Baseline are shown in parentheses. The largest and smallest flow values from each experiment are shown bold.

Model	Baseline	LUC		CC		CLUC	
cccma_cgcm3_1	237.7	235.1	(-1.1)	239.4	(0.7)	236.7	(-0.4)
cnrm_cm3	224.4	224.4	(0.0)	262.0	(16.8)	260.2	(16.0)
csiro_mk3_0	236.5	235.1	(-0.6)	246.7	(4.3)	244.5	(3.4)
csiro_mk3_5	**256.4**	**255.2**	(-0.4)	205.4	(-19.9)	204.0	(-20.4)
gfdl_cm2_0	**220.0**	**218.0**	(-1.0)	**155.0**	(-29.5)	**155.3**	(-29.4)
giss_model_e_r	235.4	232.6	(-1.2)	**278.6**	(18.3)	**276.0**	(17.2)
miub_echo_g	229.1	227.9	(-0.5)	226.8	(-1.0)	224.4	(-2.0)
mpi_echam5	246.3	244.3	(-0.8)	244.0	(-0.9)	240.0	(-2.6)
mri_cgcm2_3_2a	244.4	243.7	(-0.3)	254.0	(3.9)	250.9	(2.7)

Table 5. Simulated runoff for each land use type from the Baseline and LUC runs. The results were averaged for all GCMs.

Land use	Baseline (m^3/s)	LUC (m^3/s)	Change (m^3/s)
Water	2.55	2.44	−0.11
Developed	123.39	131.18	7.79
Barren	0.22	0.22	0.00
Forest	28.22	25.89	−2.34
Shrubland	1.77	1.62	−0.15
Herbaceous	1.90	1.78	−0.12
Planted/Cultivated	111.26	104.89	−6.37
Wetlands	30.56	29.91	−0.66
Total	299.88	297.91	−1.96

Table 6. Simulated 7Q10 (upper panel) and 7Q2 (lower panel) from different modeling experiments. Percentage changes from Baseline are shown in parentheses. The largest and smallest low flow values from each experiment are shown bold.

Model	Baseline	LUC		CC		CLUC	
cccma_cgcm3_1	36.6	35.7	(-2.5)	34.0	(-7.0)	28.6	(-21.8)
cnrm_cm3	36.3	33.3	(-8.3)	37.0	(2.1)	34.8	(-3.9)
csiro_mk3_0	23.2	**20.6**	(-11.5)	29.7	(27.9)	29.2	(25.6)
csiro_mk3_5	**21.1**	21.4	(1.2)	**6.1**	(-71.2)	**5.4**	(-74.2)
gfdl_cm2_0	31.2	28.8	(-7.6)	10.3	(-67.1)	9.0	(-71.3)
giss_model_e_r	**44.4**	41.1	(-7.4)	**63.0**	(41.9)	**61.0**	(37.4)
miub_echo_g	44.3	**44.1**	(-0.6)	21.1	(-52.3)	18.4	(-58.4)
mpi_echam5	27.9	28.4	(1.5)	36.2	(29.6)	34.1	(22.2)
mri_cgcm2_3_2a	36.9	37.1	(0.4)	42.3	(14.5)	42.3	(14.5)

Model	Baseline	LUC		CC		CLUC	
cccma_cgcm3_1	71.7	66.9	(-6.7)	65.3	(-9.0)	61.1	(-14.7)
cnrm_cm3	75.8	75.5	(-0.4)	79.7	(5.2)	75.4	(-0.5)
csiro_mk3_0	**58.8**	**59.3**	(0.8)	58.4	(-0.8)	55.0	(-6.5)
csiro_mk3_5	70.8	69.6	(-1.7)	48.0	(-32.2)	47.1	(-33.4)
gfdl_cm2_0	69.0	68.6	(-0.5)	**28.6**	(-58.6)	**27.4**	(-60.2)
giss_model_e_r	78.3	76.4	(-2.3)	**94.0**	(20.1)	**92.0**	(17.6)
miub_echo_g	71.5	66.7	(-6.6)	51.2	(-28.4)	48.5	(-32.1)
mpi_echam5	75.5	74.5	(-1.3)	82.7	(9.6)	77.3	(2.5)
mri_cgcm2_3_2a	**78.9**	**77.5**	(-1.8)	86.6	(9.7)	81.2	(2.9)

Figures

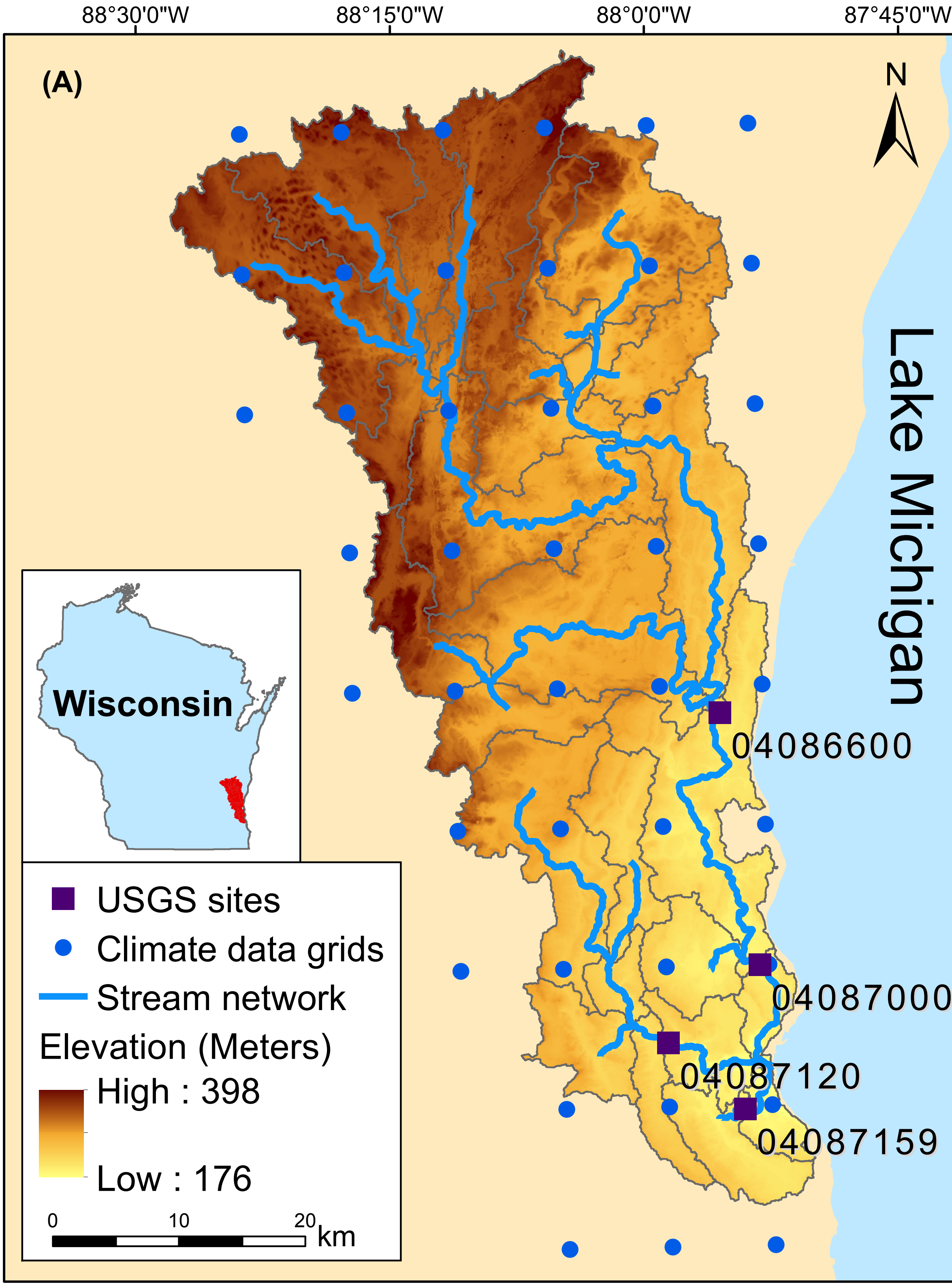
88°30'0"W
88°15'0"W
88°0'0"W
87°45'0"W
43°40'0"N
43°30'0"N
43°20'0"N
43°10'0"N
43°0'0"N
(A)
N
Lake Michigan
Wisconsin
04086600
04087000
04087120
04087159
USGS sites
Climate data grids
Stream network
Elevation (Meters)
High : 398
Low : 176
0
10
20
km

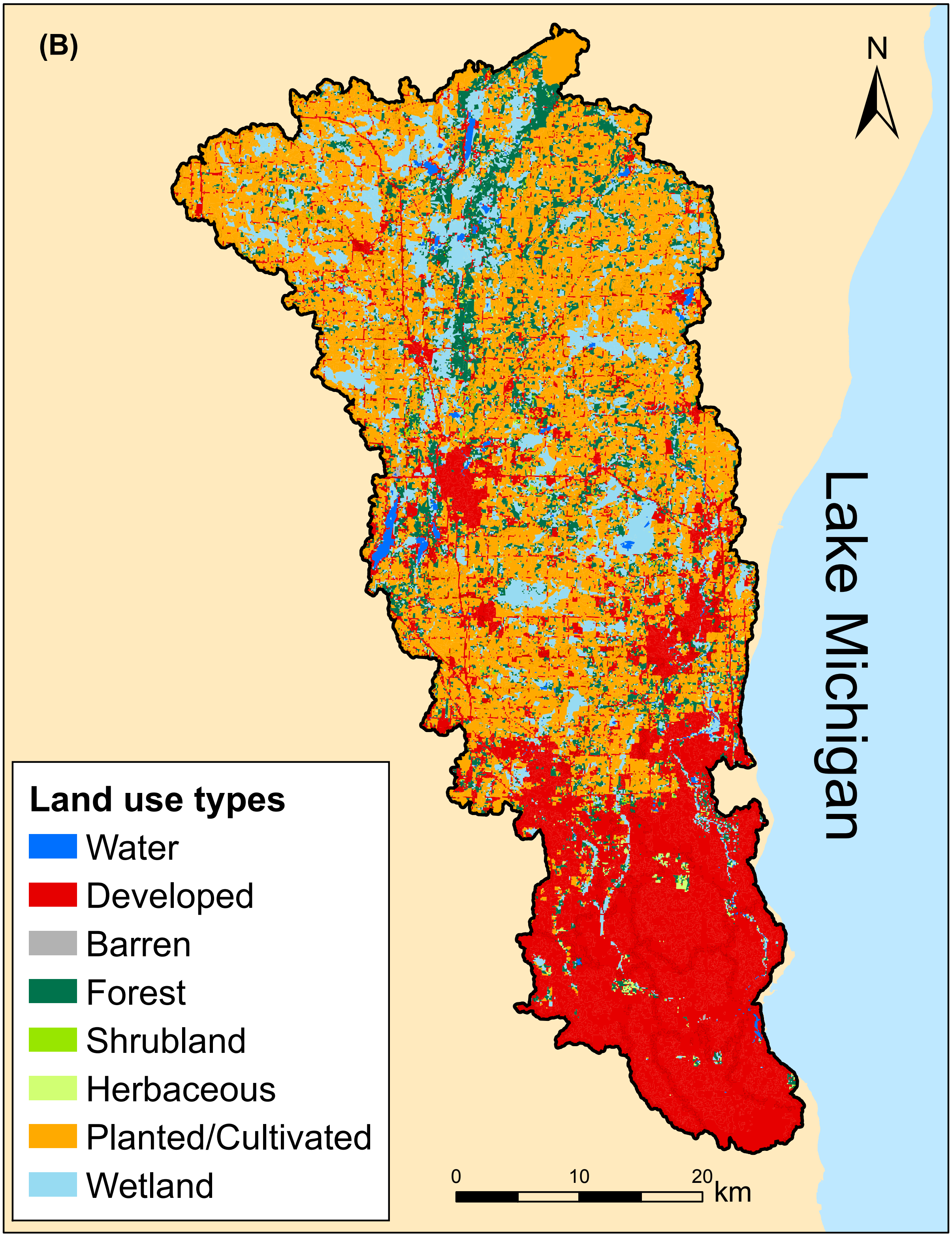

Figure 1. (A) The boundary, major streams, and elevations of the Milwaukee River catchment. Its location in the state of Wisconsin is shown in the inset map. Also shown are the grid points of the historical climate data and the U.S. Geological Survey (USGS)

streamflow measurement sites. Details for the sites are available in Table 1 of the Electronic Supplementary Material (B) Land use of the Milwaukee River catchment from NLCD 2001

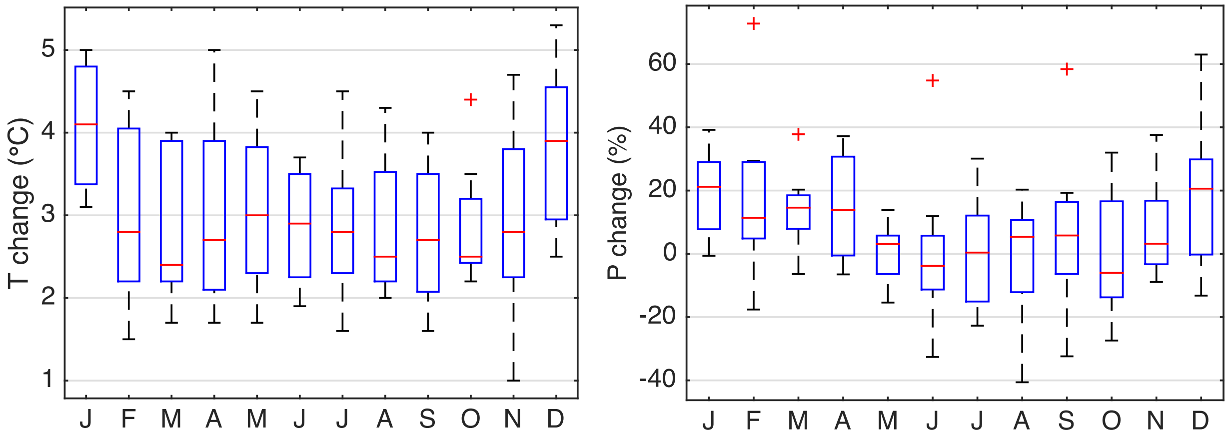

Figure 2. Distribution of mean monthly changes in temperature and precipitation between 1961-2000 and 2046-2065 projected by the nine GCMs. The horizontal lines within the boxes indicate lower quartile, median, and upper quartile values. Whiskers represent the most extreme values within 1.5 times the interquartile range. Plus (+) signs denote outliers. Same for other box-whisker plots.

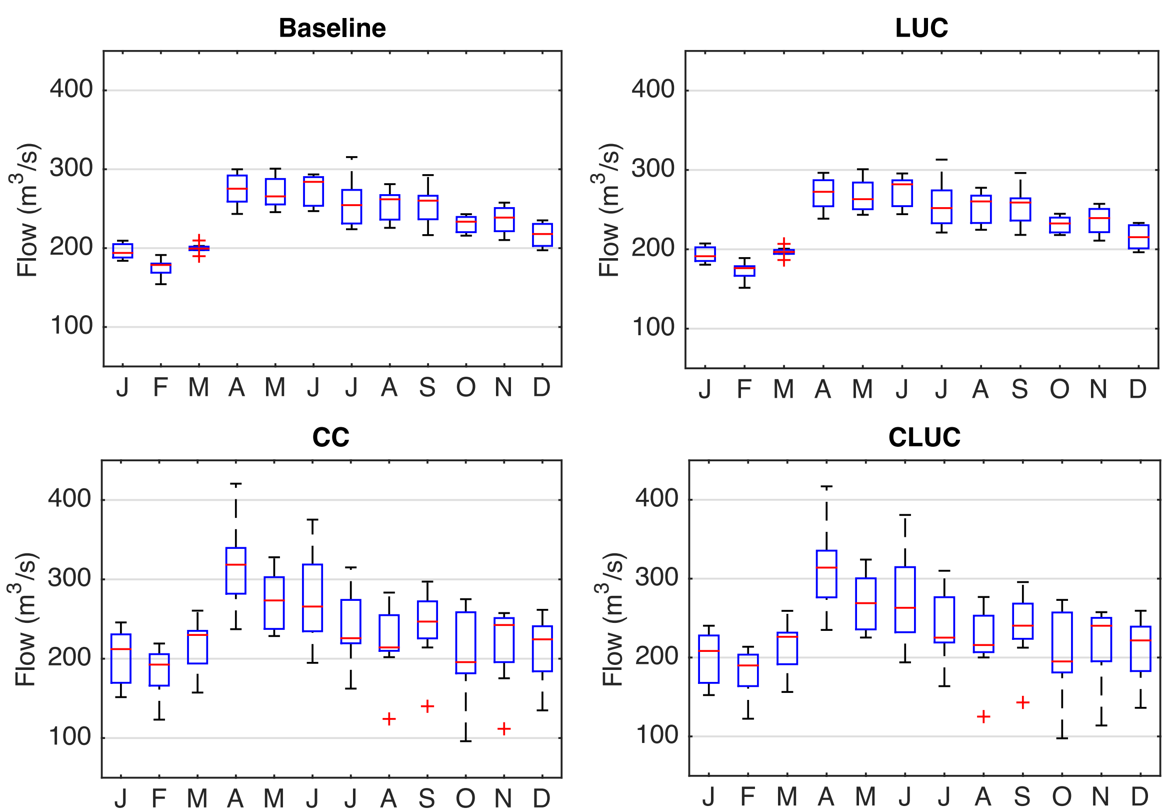

Figure 3. Distribution of simulated mean monthly streamflow according to the nine GCMs.

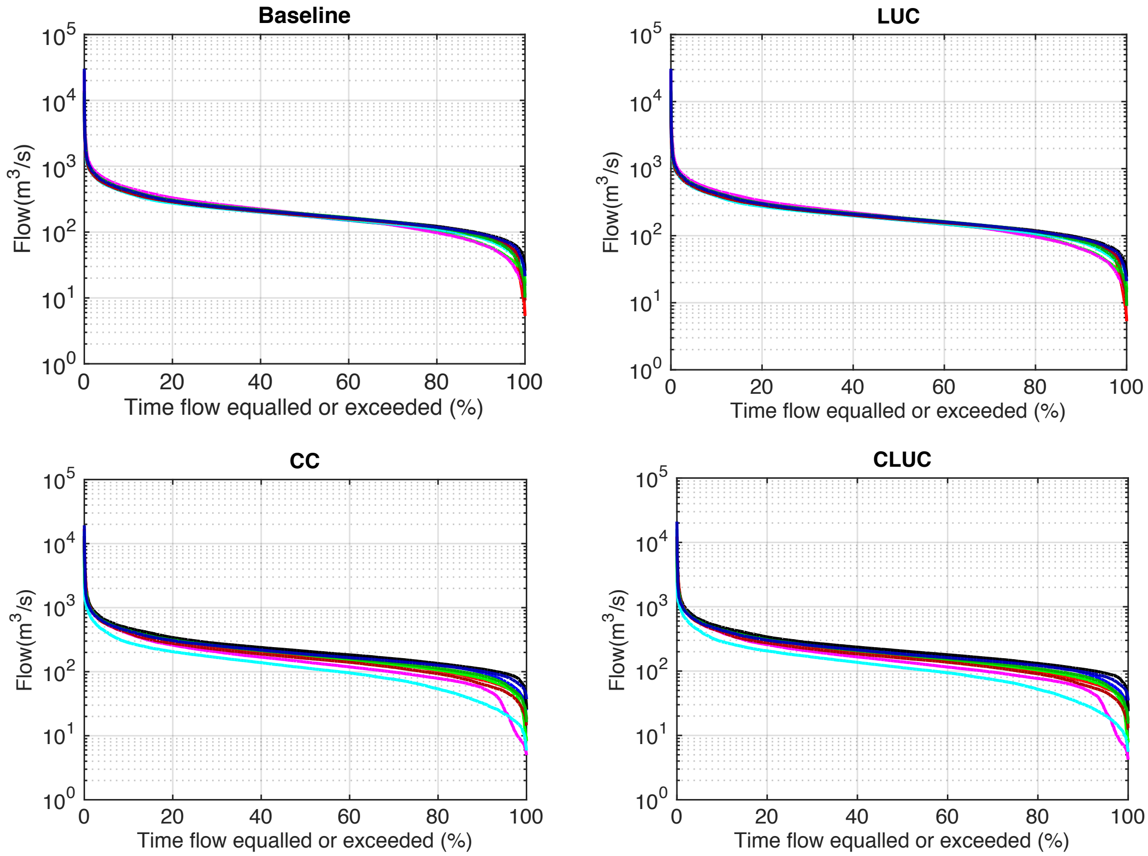

Figure 4. Daily flow duration curves from the simulation Baseline, LUC, CC, and CLUC. The lines of different colors indicate different GCMs.